A RAMAN SPECTROSCOPY STUDY OF TAUTOMERIC O–H···O HYDROGEN BONDING

B. A. Kolesov[1]*

The work reports a study of the properties of tautomeric O–H···O hydrogen bonding (τ-bonding). The Raman spectra of crystalline and polycrystalline samples of terephthalic acid chains, benzoic acid dimers, and ibuprofen dimers are studied in the temperature region of 5-300 K. The protons on τ-bonds in terephthalic acid and ibuprofen are substituted by deuterium. Temperature dependences of the frequencies of τ-bond translational vibrations are analyzed, their relation to tunneling and proton hopping is discussed. It is shown that the propagation of the proton (deuteron) density distribution function into the neighboring empty potential well increases hydrogen bonding, while physical motion of the particle through the barrier or hopping over the barrier affect the $\omega(T)$ dependence of the vibration of the C=O bond in the τ-ring. On the example of ibuprofen, asymmetric τ-bonds are analyzed and the energy difference between L- and R-tautomers are measured.

INTRODUCTION

Proton tautomerism occurs in the systems containing intermolecular hydrogen bonds X–H···X where the donor and the acceptor are indistinguishable so that the proton can jump between them. The simplest compound with tautomeric bonds (τ-bonds) is the formic acid dimer (Fig. 1) whose left (L-) and right (R-) tautomers are identical, while two hydrogen bonds and the dimer's carboxyl groups form a six-membered τ-ring.
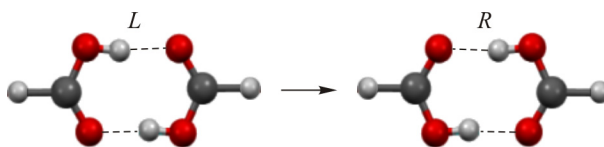

Fig. 1. L- and R-tautomers in formic acid dimers.

The potential function of the proton along the τ-bond is a curve with two identical potential wells (Fig. 2a). In the presence of a symmetric double-well potential, the protons should be able to jump in a concerted manner between the wells, as is actually the case when the protons jump over or tunnel through the potential barrier. However, the symmetric double-

[1]Nikolaev Institute of Inorganic Chemistry, Siberian Branch, Russian Academy of Sciences, Novosibirsk, Russia; *kolesov@niic.nsc.ru. Original article submitted March 27, 2020; revised April 14, 2020; accepted April 14, 2020.
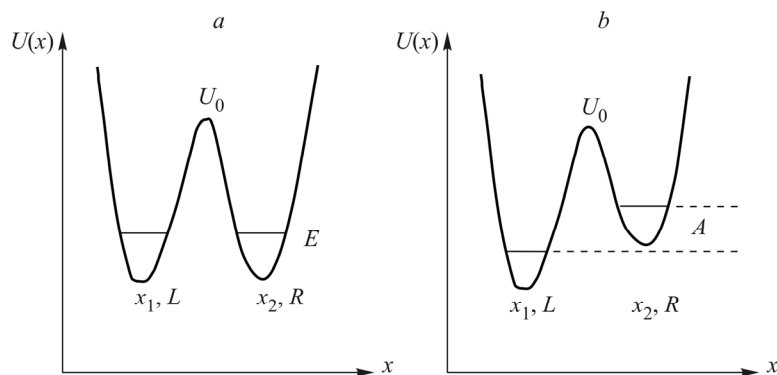
Fig. 2. Potential energy of the proton on the τ-bond of an isolated dimer (trimer, etc.) in the gas phase (*a*), the same energy of a real dimer in the crystal (*b*). Particle energy in the potential well (*E*), barrier height (U_0), coordinates of potential energy minima (x_1, x_2). *A* is the difference between the energies of *L*- and *R*-tautomers in the crystal lattice.

well potential is realized only for isolated molecular formations in the gas phase. In the crystal, the coordinated transition of charge-carrying protons to the next potential well affects the interaction between the given τ-ring and the τ-ring of the neighboring molecule where this transition is not yet completed. In other words, the energies of *L*- and *R*-tautomers in the crystal lattice differ by the value *A* (Fig. 2*b*). Therefore, the tunneling must be accompanied by the absorption of the phonon ω_A ($\hbar\omega_A = A$), and the temperature dependence of the tunneling rate is determined by the average value of the vibrational quantum number of phonons ω_A and is anti-Stokes in nature.

The structures of compounds with τ-bonding are diverse and include crystals with infinite chains, dimers, trimers, and tetramers [1]. Moreover, both the same type atoms (O–H⋯O, N–H⋯N) and different type atoms (O–H⋯N, N–H⋯O) can be donors and acceptors in tautomeric hydrogen bonds. Proton transfer along τ-bonds has been broadly studied by pulsed NMR spectroscopy and inelastic neutron scattering [2-12]. A theory of coordinated motion of protons on τ-bonds was developed in [6].

The present work is an attempt to obtain the data on the behavior of protons on τ-bonds using simple and easily available Raman spectroscopy. For this purpose, Raman spectra of compounds with symmetric (chains of terephthalic acid, $C_8H_6O_4$, TPA, Fig. 3*a*), quasisymmetric (benzoic acid dimers, C_6H_5COOH, BZ, Fig. 3*b*), and asymmetric (ibuprofen dimers, $C_{13}H_{18}O_2$, IB, Fig. 3*c*) τ-bonds were considered in a temperature region of 5-300 K.
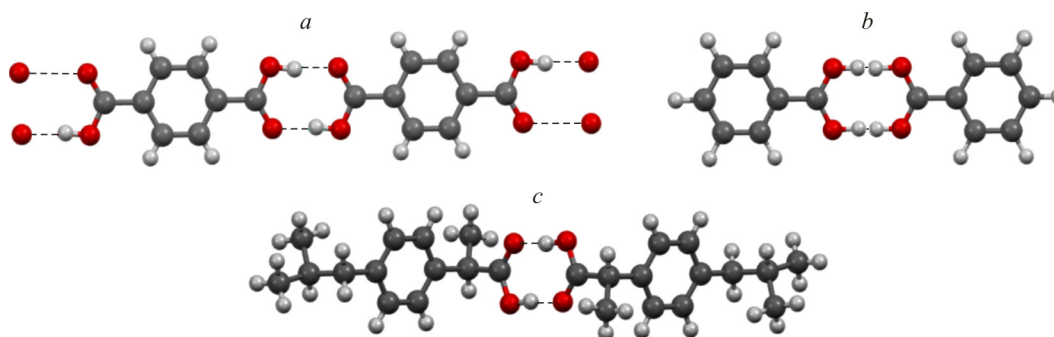

Fig. 3. Chains of TPA molecules with symmetric τ-bonding (*a*), BZ dimers with quasisymmetric τ-bonding (*b*), and IB dimers with asymmetric τ-bonding (*c*). A slight deviation from perfect symmetry in the benzoic acid dimer is due to the crystalline effect making one of four oxygen atoms of the τ-bond have a shorter contact with the environment than the contacts with three other oxygen atoms. The asymmetry of the IB dimer is due to two different substituents of the carbon atom next to the alpha carbon of the hydroxyl group.

EXPERIMENTAL

The studied single- and polycrystals were prepared from commercially available reagents. The structures were taken from the Cambridge Structural Database.

TPA and IB were deuterated according to the procedure described in [13] so that only hydrogen atoms of the τ-bonds were substituted.

The spectra were collected on a LabRAM Horiba HR spectrometer with a CCD Symphony (Jobin Yvon) detector with 2048 horizontal pixels. The laser power (633 nm line of He–Ne laser, 514 nm and 488 nm lines of Ar^+ laser) on the sample surface did not exceed 3 mW. The spectra at all temperatures were measured in the backscattering collection geometry with a Raman microscope. To collect Raman spectra at different temperatures, the sample was wrapped in an indium foil for better thermal contact and placed on the cold finger of a closed-cycle helium cryostat. All measurements were performed with a spectral resolution of 0.3–0.7 cm^{-1}. The measurements that required high accuracy of determining Raman frequency shifts at varying temperatures of the sample were conducted with a He-Ne laser only. For better accuracy of determining small vibration frequency shifts during temperature measurements, all spectra were corrected with respect to the position of the emission line of a Ne lamp registered simultaneously with the Raman spectrum of the compound (Fig. 7a). After the measurement, all spectra were numerically processed to determine spectral parameters (peak position, band half-width, and integral intensity) for each vibrational mode.

Quantum chemical calculations of isolated four-link TPA(H) and TPA(D) chains, as well as the isolated ibuprofen dimers were performed with the Gaussian 09 package [14], and the obtained results were reported in [13, 15]. Optimized geometries and vibrational frequencies of compounds were calculated using B3LYP/6-31G and M06-2X/6-31+G hybrid methods of the density functional theory. Both these methods gave similar results.

RESULTS AND DISCUSSION

The behavior of protons on the τ-bond is quite complicated and is characterized by several independent processes.

1.   At large $d_{O \cdots O}$ distances (> 2.6 Å), a coordinated proton transition along the τ-bond occurs mainly due to proton hopping over the potential barrier U_0 with the participation of phonons $\hbar \omega_U \sim U_0$ (phonon-assisted hopping). Back and forth hopping between L- and R-tautomers does not change the length and the strength of hydrogen bonding, but it switches the positions of C–O and C=O bonds in the carboxyl groups. Therefore, the main effect of proton hopping is manifested exactly in the behavior of vibration frequencies of these two bonds.

2.   At low temperatures, the $d_{O \cdots O}$ distance becomes extremely short and the barrier becomes extremely low for this compound due to the freezing of vibrations. As a result, both protons on the τ-bond of compounds with strong hydrogen bonds ($d_{O \cdots O} < 2.6$ Å) can undergo coordinated transitions by tunneling through the barrier. Tunneling, similar to proton hopping, does not change the force constant of the τ-bond but makes C–O and C=O bonds switch between each other. In this case, the length of these two bonds are changed with the frequency of tunneling, which is usually equal to $\sim 10^9$ s^{-1} [7], while the bond lengths are changed with amplitudes that are approximately one order of magnitude larger than those of equilibrium (thermal) vibration of these bonds. For this reason, both proton tunnelling and proton hopping cause forced vibrations of C–O and C=O bonds of carboxyl groups so that the frequencies of their normal vibrations demonstrate an anharmonic shift [13]. Thus, temperature dependence of C–O or C=O stretchings is an indicator of both proton tunneling through the barrier and proton hopping over the barrier U_0. The tunneling rate is significantly reduced due to deuteration, since its probability is proportional to $\exp(-B\sqrt{m})$, where m is the mass of the tunneling particle; B is a constant.

3.   The proton density distribution function is delocalized in the potential well due to quantum uncertainty and partially propagates into the neighboring (empty) well. This function was described in the works by Benoit and Marx [16] and Wang et al. [17] and is shown schematically in Fig. 4. The proton density that propagates into the neighboring empty
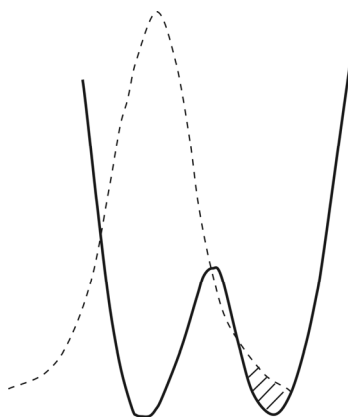
Fig. 4. Hypothesized proton density distribution (dashed curve) for $d_{O \cdots O} < 2.6$ Å. The shaded area shows the region where the proton density propagates into the neighboring well.

well must form covalent bonding with the acceptor oxygen in the same way as with the donor oxygen (Fig. 4). As a result, the strength of the hydrogen bond and the frequency of translational vibrations ω_τ (i.e. vibrations of two components of the τ-ring relative to each other) should increase. The proton density propagation is increasing for smaller $d_{O \cdots O}$ distances and temperatures of the crystal. Wang et al. [17] also showed that quantum uncertainty of the deuterium atom on the bond differs only slightly from that of the proton.

Note that in contrast to hopping and tunneling, where the coordinated transition of protons to the neighboring well takes place in an arbitrary τ-ring of the lattice and independently on the environment, the propagation of the proton density to the neighboring potential minimum occurs simultaneously and similarly in all τ-rings of the lattice and therefore does not change the energy state of protons in the neighboring rings. In other words, the scheme in Fig. 2b is not true in the case of delocalized proton density.

Thus, when analyzing the experimental data, we will proceed from the following assumptions.

1. Coordinated proton tunneling on the τ-bond occurs mainly at low temperatures, while proton hopping occurs mainly at high temperatures.

2. The transition of protons to the neighboring well as a result of tunneling changes the energy of their interaction with the environment and requires the participation of phonons ω_A (Fig. 2b).

3. The propagation of the proton density to the neighboring well (Fig. 4) strengthens the hydrogen τ-bond and does not change the proton energy (Fig. 2a).

4. Proton tunneling and hopping do not affect the force constant of the τ-bond but modulate the length of C–O and C=O bonds of the τ-ring.

5. Deuteration of the τ-bond virtually does not change the amount of proton density penetrating to the neighboring well (Fig. 4) but significantly slows down the tunneling process.

Thus, the modes of translational vibrations of the τ-bond, ω_τ, and the vibration of the C=O bond of the τ-ring (the C–O vibration mode is more difficult to analyze) are most important and informative for the analysis of hopping and tunneling. The experimental assignment of spectral lines to the translational vibrations was done for all compounds using temperature dependence of corresponding frequencies and quantum chemical calculations. In the case of terephthalic acid and ibuprofen, the assignment was additionally confirmed by the deuteration on the τ-bond [13, 15]. The structural parameters of O–H$\cdots$O τ-bonds and experimental and calculated frequencies ω_τ are listed in the Table 1.

Quantum delocalization of protons. Fig. 5 shows temperature dependences of peaks positions of translational modes in three different compounds.

TABLE 1. Hydrogen Bond Lengths and Vibrational Frequencies ω_τ in the Studied Compounds

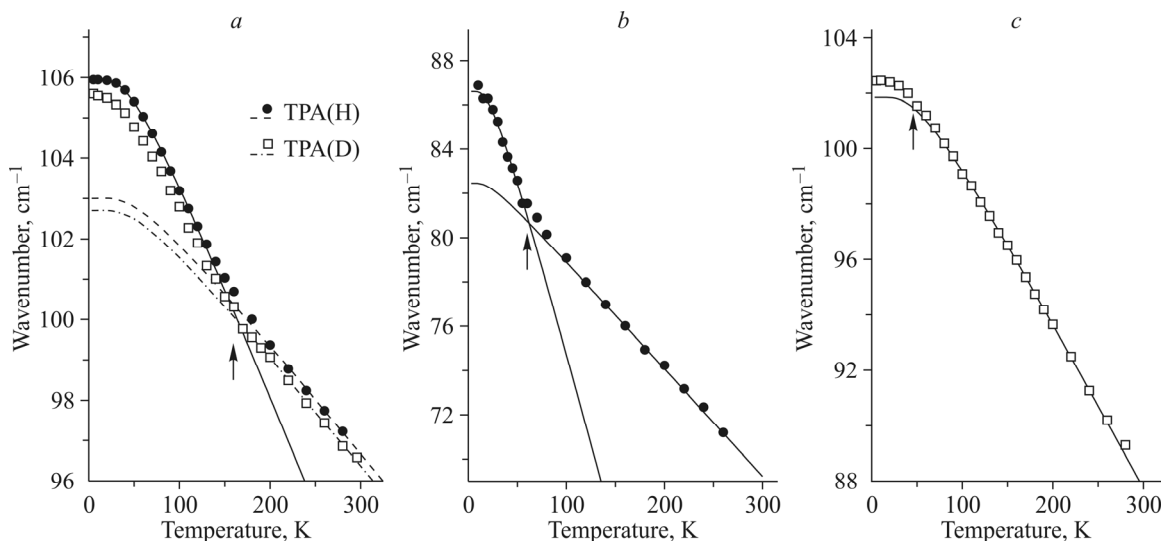| Compound	$d_{O \cdots O}$, Å	ω_τ, cm^{-1}	
		Calculation [13, 15]	Experiment, 5 K
TPA(H)	2.62 [18]	114	106
TPA(D)		113	105
BZ	2.63 [19]	–	86
IB(H)	2.66 [20]	108	103.93
IB(D)		–	102.90

Fig. 5. Temperature dependences of the frequency of translational vibrations ω_τ in symmetric TPA(H) and TPA(D) (*a*), quasisymmetric BZ (*b*), and asymmetric IB (*c*) tautomeric bonds. Solid curves are plotted taking into account the anharmonic shift of phonon ω determined by its thermal population [21]. The arrows show kink points on the $\omega_\tau(T)$ dependence curve. Low- and high-temperature parts of the curves in Fig. *a*, *b* are shown by blue and red dots and curves, respectively.

The temperature dependence $\omega_\tau(T)$ of symmetric τ-bond in TPA (Fig. 5*a*) has a characteristic kink point whose position on the temperature scale correlates with the beginning of the freezing of translational vibrations, i.e. the temperature where the average value of the quantum number *n* of the mode at 106 cm^{-1} becomes smaller than unity. The kink point in the temperature dependence $\omega_\tau(T)$ is also observed in the crystals with symmetric N–H$\cdots$N τ-bonds [22]. In the quasisymmetric τ-bond in BZ (Fig. 5*b*), there is also a kink point in the $\omega_\tau(T)$ dependence, but it corresponds to a lower temperature than the beginning of phonon freezing (87 cm^{-1}). Finally, in the asymmetric case of IB (Fig. 5*c*), the kink on the temperature dependence $\omega_\tau(T)$ is negligible and is observed at $T < 50$ K.

Based on dependence $\omega_\tau(T)$ for the symmetric τ-bond in TPA (Fig. 5*a*), it can be assumed that the transition of the vibrational state of the translation mode from the excited state ($n = 1$) to the ground state ($n = 0$) diminishes the $x_1 - x_2$ distance between potential minima (Fig. 2) by increasing the degree of propagation of proton density from the filled potential well to the empty well and by strengthening the hydrogen bond. As can be seen in Fig. 5, the slope of the $\omega_\tau(T)$ curve in TPA(D) starts changing virtually at the same temperatures as in TPA(H). This experiment conclusively confirms the above assumption that low-temperature changes of the frequency of translational vibrations are associated with the propagation of proton (deuteron) wave function to the neighboring well rather than with physical proton motions, since the tunneling

probability in the latter case would be significantly diminishing with increasing mass of the tunneling particle (see more details in [23]).

As can be seen from Fig. 5, the higher the symmetry of the τ-bond, the higher the temperature corresponding to the kink point on the $\omega_\tau(T)$ dependence. This means that the degree of proton delocalization is maximal for strictly symmetrical τ-bonds (Fig. 2a), i.e. in TPA. Indeed, the slope of the $\omega_\tau(T)$ curve could change for any hydrogen bond X–H$\cdots$Y with a sufficiently small distance X$\cdots$Y; however, this distance is itself depending on the symmetry of the bond, i.e. on how close the donor and the acceptor are in terms of their chemical state (proton affinity).

Proton hopping in ibuprofen. IB (Fig. 3c) is an example of asymmetric τ-bonding. In this case, left- and right-tautomers are initially unequal in terms of energy states and are characterized by the energy difference ΔE. For this reason, the degree of proton propagation in the neighboring minimum is very small in IB, and proton tunneling should be negligibly weak. Since proton tunneling and protons hopping are equally manifested in structural and energy characteristics of compounds, the registration of proton hoping in IB spectra is greatly facilitated in the absence of tunneling.

At low temperatures, the translation vibration of the IB τ-bond is represented by a single mode at ~103 cm^{-1} corresponding to the L-tautomer; an additional band appearing above 150 K at 90 cm^{-1} corresponds to translational vibrations of the R-tautomer [13].

The temperature dependences of these two intensities (the modes at ~ 100 cm^{-1} and at ~ 90 cm^{-1}) show a pronounced activation character, i.e. demonstrate two τ-bond states separated by the energy ΔE equal to 80 meV in the normal crystal and to 70 meV in the deuterated crystal [13].

However, the significance of registering proton transitions from L- to R-states in IB is not related to the determination of energy ΔE; rather, it is related to the possibility of determining spectral characteristics to describe proton hopping.

Fig. 6 shows the temperature dependence of the C=O stretching vibration in the carboxyl group of the ibuprofen dimer. On the one hand, as the temperature grows from 5 K, the stretching vibration frequency of the C=O bond of the L-tautomer (only L-tautomers exist at low temperatures) should decrease as a result of usual anharmonic processes. On the other hand, the frequency should increase, since the same anharmonic processes diminish the participation of the terminal C=O group in the hydrogen O-H$\cdots$O=C bonding, which is always accompanied by the increase of the C=O frequency. Fig. 6 shows that the second process is somewhat more effective and that $\omega_{C=O}$ is slightly increased in the temperature region of 5–150 K. However, at $T \geq 150$ K, the frequency $\omega_{C=O}$ unexpectedly decreases, and the exponential factor of the frequency change is the same as in the activation of the R-tautomer, i.e. ~80 meV (Fig. 6). In other words, the change of $\omega_{C=O}$ strictly correlates with the appearance of the R-tautomer both in terms of temperature and in terms of the change rate. The reason for the unusual behavior of the $\omega_{C=O}$ mode is the following. The back and forth transitions between L- and R-tautomers make the carboxyl C–O and C=O bonds switch their places. The ordinary C–O bond becomes a double bond and is substantially shortened (by ~ 0.1 Å), while the double C=O bond is elongated by the same value. This process proceeds with the frequency of proton hopping on the τ-bond, i.e. 10^8-10^{11} s^{-1} in the temperature region of 5-300 K (e.g., see [9-12]). Thus, the bond lengths in the carboxyl group are subject to forced vibrations which occur with a frequency of proton hopping and with a very high amplitude that several times exceeds the amplitude of normal vibrations. The forced vibrations of the carboxyl group cause the same anharmonic phenomena as normal vibrations. As a result, the C=O bond elongates and the frequency of normal vibrations starts decreasing as a result of proton hopping, as can be seen in Fig. 6. Thus, the $\omega_{C=O}(T)$ dependence can be used as a high-sensitive method to characterize proton hopping at high temperatures and proton tunneling in the systems with τ-bonds. To our knowledge, no forced vibrations of chemical bonds with an arbitrary frequency have been observed before. Therefore, this phenomenon can be related to a new type of forced vibrations.

The temperature dependence in Fig. 6 also confirms the above conclusion that no tunneling takes place in IB at low temperatures of 5-150 K.
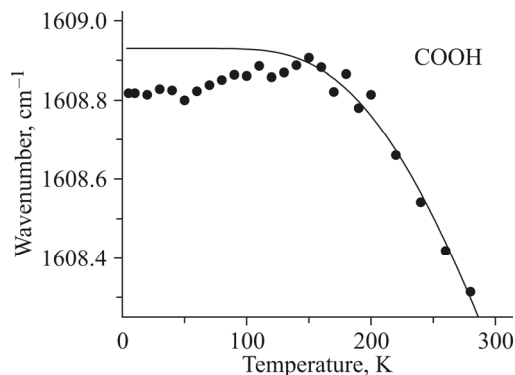
Fig. 6. Temperature dependence of the peak position of the 1609 cm^{-1} band of C=O stretchings (dots). The solid curve is plotted under the condition that the vibration frequency is changed due to the activation process with ΔE=80 meV.
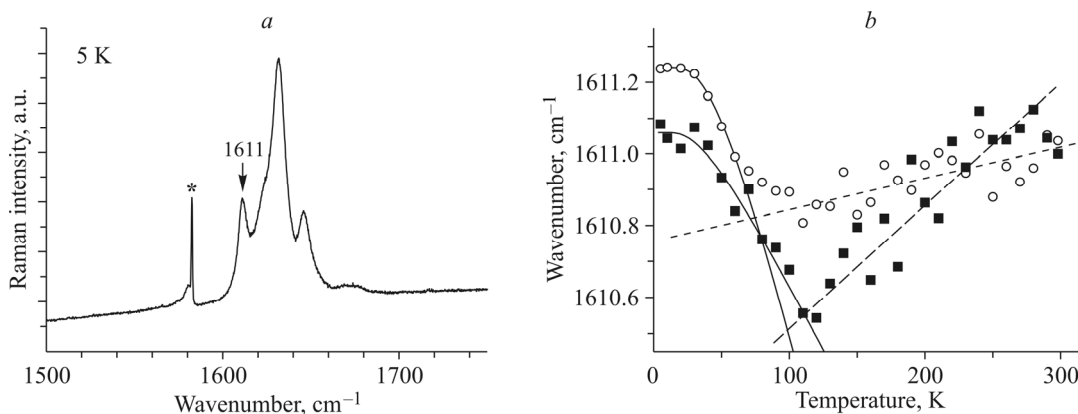

Fig. 7. Spectrum of TPA(H) at 5 K in the region of C=O vibrations. The asterisk marks the position of the neon lamp line which was recorded at each temperature for the spectra correction (*a*); temperature dependence of the C=O vibrational frequency of COOH (empty circles) and COOD (black squares). The solid line is proportional to the thermal population of phonons ω_A (see the text); the dashed lines for temperatures above 100 K are drawn approximately.

Proton tunneling. The described experiment with the frequency of C=O vibrations has no particular importance for ibuprofen, since the process of proton hopping is clearly demonstrated by the dependence of the intensities of translational modes in the crystal [13]. However, it is a very sensitive tool to characterize both proton hopping and proton tunneling to the neighboring well in other compounds such as TPA chains with symmetric τ-bonds.

As it was mentioned above, the coordinated motion of protons to the neighboring potential well must be accompanied by the absorption of the phonon ω_A ($\hbar\omega_A = A$, Fig. 2*b*), and the temperature dependence of the tunneling rate is determined by the average value of the vibrational quantum number of phonon ω_A and is anti-Stokes in nature.

Fig. 7*b* shows the dependences of the frequencies of C=O stretching vibrations in carboxyl groups of TPA(H) and TPA(D) compounds. In this case, the anharmonic shift of $\omega_{C=O}$ is proportional to the tunneling rate and is associated with the energy change by the value of A at low temperatures and with proton hopping over the barrier U_0 at high temperatures. The solid lines show the dependences of the 1611 cm^{-1} mode of C=O stretching vibrations at low temperatures and are drawn according to the expression $\omega_{C=O}(T) = \omega_{C=O}(0) - C\langle n \rangle$, where $\langle n \rangle$ is the average quantum number of the phonon ω_A and C is a proportionality constant.

As can be seen from Fig. 7*b*, *A* is equal to ~12 meV in TPA(H) and to ~9 meV in TPA(D). The proportionality constant *C* is 2.2 cm^{-1} in TPA(H) and 0.75 cm^{-1} in TPA(D). The latter fact suggests that the probability of proton tunneling is significantly higher than that of deuteron tunneling, in agreement with theoretical concepts. A slight linear increase of frequency $\omega_{C=O}$ at *T* > 100 K in both compounds (dashed lines in Fig. 7*b*) is due to the fact that the hydrogen τ-bond weakens at elevated temperatures and the tunneling is gradually terminated. It testifies that the hopping rate is low in TPA(H) and is still lower in TPA(D). Possibly, no hopping takes place in the latter case at all. It should be noted that numerical values of barrier *A* and the fact that no high rate hopping occurs at elevated temperatures disagree with the data of [7] where *A* and the barrier U_0 were reported to be 16.25 meV (130 cm^{-1}) and 75 meV (600 cm^{-1}), respectively.

CONCLUSIONS

The Raman spectra of compounds with tautomeric O-H⋯O hydrogen bonding in the temperature region of 5-300 K perfectly illustrate the behavior of protons on τ-bonds. The spectra allow separating different mechanisms of proton density distribution by temperature so that hopping and tunneling processes can be studied using simple and available Raman spectroscopy. The results presented in this paper largely coincide with those reported previously in [2-12]. However, we believe that the description of proton behavior on τ-bonds obtained here using Raman spectroscopy supplement the works based on the methods of nuclear magnetic resonance (NMR) and inelastic scattering (INS). Undoubtedly, the two latter methods provide highly reliable data, but they can register only the final phase of tunneling associated with proton transition between the wells. In addition, protons are ordered on τ-bonds at very low temperatures, and the tunneling rate is low. In this case, the relaxation time T_1 is too large to be registered by NMR, and the INS signal also becomes too weak. Therefore, none of this techniques can be used at very low temperatures [6]. Also, the change in the energy of the process (in this case, vibrational frequency), which can be registered in Raman experiments, is of the order of tenths of an inverse centimeter (hundredths of millielectronvolts), which seems to be beyond the capabilities of NMA and INS methods.

CONFLICT OF INTERESTS

The author declares that he has no conflict of interests.

REFERENCES

1. C. Foces-Foces, A. Echevarría, N. Jagerovic, I. Alkorta, J. Elguero, U. Langer, O. Klein, M. Minguet-Bonveh, and H-H. Limbach. *J. Am. Chem. Soc.*, **2001**, *123*, 7898–7906.
2. S. Nagaoka, T. Terao, F. Imashiro, A. Saika, N. Hirota, and S. Hayashi. *Chem. Phys. Lett.*, **1981**, *80*, 580–584.
3. B. H. Meier, F. Graf, and R. R. Ernst. *J. Chem. Phys.*, **1982**, *76*, 767–774.
4. B. H. Meier, R. Meyer, R. R. Ernst, P. Zolliker, A. Furrer, and W. Hälg. *Chem. Phys. Lett*, **1983**, *103*, 169–174.
5. S. Nagaoka, T. Terao, F. Imashiro, A. Saika, N. Hirota, and S. Hayashi. *J. Chem. Phys.*, **1983**, *79*, 4694–4703.
6. J. L. Skinner and H. P. Trommsdorff. *J. Chem. Phys.*, **1988**, *89*, 897–907.
7. A. J. Horsewill and A. Aibout. *J. Phys.: Condens. Matter*, **1989**, *1*, 9609–9622.
8. A. J. Horsewill, A. Ikram, and I. B. I. Tomsah. *Mol. Phys.*, **1995**, *84*, 1257–1272.
9. D. F. Brougham, A. J. Horsewill, A. Ikram, R. M. Ibberson, P. J. McDonald, and M. Pinter-Krainer. *J. Chem. Phys.*, **1996**, *105*, 979–982.
10. D. F. Brougham, A. J. Horsewill, and R. I. Jenkinson. *Chem. Phys. Lett.*, **1997**, *272*, 69–74.
11. M. Neumann, F. Brougham, C. J. McGloin, M. R. Johnson, A. J. Horsewill, and H. P. Trommsdorff. *J. Chem. Phys.*, **1998**, *109*, 7300–7311.

12. A. J. Horsewill, C. J. McGloin, H. P. Trommsdorff, and M. R. Johnson. *Chem. Phys*., **2003**, *291*, 41–52.

13. A. G. Demkin and B. A. Kolesov. *Phys. Chem. A*, **2019**, *123*, 5537–5541.

14. M. J. Frisch, G. W. Trucks, H. B. Schlegel, G. E. Scuseria, M. A. Robb, J. R. Cheeseman, G. Scalmani, V. Barone, B. Mennucci, G. A. Petersson, H. Nakatsuji, M. Caricato, X. Li, H. P. Hratchian, A. F. Izmaylov, J. Bloino, G. Zheng, J. L. Sonnenberg, M. Hada, M. Ehara, K. Toyota, R. Fukuda, J. Hasegawa, M. Ishida, T. Nakajima, Y. Honda, O. Kitao, H. Nakai, T. Vreven, J. A. Montgomery Jr., J. E. Peralta, F. Ogliaro, M. Bearpark, J. J. Heyd, E. Brothers, K. N., Kudin, V. N. Staroverov, R. Kobayashi, J. Normand, K. Raghavachari, A. Rendell, J. C. Burant, S. S. Iyengar, J. Tomasi, M. Cossi, N. Rega, J. M. Millam, M. Klene, J. E. Knox, J. B. Cross, V. Bakken, C. Adamo, J. Jaramillo, R. Gomperts, R. E. Stratmann, O. Yazyev, A. J. Austin, R. Cammi, C. Pomelli, J. W. Ochterski, R. L. Martin, K. Morokuma, V. G. Zakrzewski, G. A. Voth, P. Salvador, J. J. Dannenberg, S. Dapprich, A. D. Daniels, O. Farkas, J. B. Foresman, J. V. Ortiz, J. Cioslowski, and D. J. Fox. Gaussian 09, Revision A.01. Gaussian, Inc. Wallingford, CT, 2009.

15. E. A. Pritchina and B. A. Kolesov. *Spectrochim. Acta, Part A*, **2018**, *202*, 319–323.

16. M. Benoit and D. Marx. *ChemPhysChem*, **2005**, *6*, 1738–1741.

17. L. Wang, S. D. Fried, S. G. Boxer, and T. E. Markland. *PNAS*, **2014**, *111*, 18454–18459.

18. P. Fischer, P. Zolliker, B. H. Meier, R. R. Ernst, A. W. Hewat, J. D. Jorgensen, and F. J. Rotella. *J. Solid State Chem*., **1986**, *61*, 109–125.

19. C. C. Wilson, N. Shankland, and A. J. Florence. *Chem. Phys. Lett*., **1996**, *253*, 103–107.

20. K. Ostrowska, M. Kropidłowska, and A. Katrusiak. *Cryst. Growth Des*., **2015**, *15*, 1512–1517.

21. B. A. Kolesov. *J. Raman Spectrosc*., **2017**, *48*, 323–326.

22. Yu. A. Galkina, M. A. Vershinin, and B. A. Kolesov. *J. Struct. Chem*., **2019**, *60(3)*, 398–404.

23. B. A. Kolesov. *J. Phys*. *Chem*. *Solids*, **2020**, *138*, 1092888.